BIOCHEMISTRY

DNA topology in chromatin is defined by nucleosome spacing

Tatiana Nikitina,[1] Davood Norouzi,[1] Sergei A. Grigoryev,[2]* Victor B. Zhurkin[1]*

In eukaryotic nucleosomes, DNA makes ~1.7 superhelical turns around histone octamer. However, there is a long-standing discrepancy between the nucleosome core structure determined by x-ray crystallography and measurements of DNA topology in circular minichromosomes, indicating that there is only ~1.0 superhelical turn per nucleosome. Although several theoretical assumptions were put forward to explain this paradox by conformational variability of the nucleosome linker, none was tested experimentally. We analyzed topological properties of DNA in circular nucleosome arrays with precisely positioned nucleosomes. Using topological electrophoretic assays and electron microscopy, we demonstrate that the DNA linking number per nucleosome strongly depends on the nucleosome spacing and varies from −1.4 to −0.9. For the predominant {10*n* + 5} class of nucleosome repeats found in native chromatin, our results are consistent with the DNA topology observed earlier. Thus, we reconcile the topological properties of nucleosome arrays with nucleosome core structure and provide a simple explanation for the DNA topology in native chromatin with variable DNA linker length. Topological polymorphism of the chromatin fibers described here may reflect a more general tendency of chromosomal domains containing active or repressed genes to acquire different nucleosome spacing to retain topologically distinct higher-order structures.

INTRODUCTION

In eukaryotic chromatin, the DNA double helix is repeatedly supercoiled in the nucleoprotein particles called nucleosomes. The core of a typical nucleosome contains 145 to 147 base pairs (bp) of DNA making 1.7 left-handed superhelical turns around a histone octamer (*1*–*3*). The nucleosomes play an essential role in regulating all DNA-dependent processes such as transcription, replication, recombination, and repair through local and dynamic unfolding of chromatin (*4*–*6*).

In the cell nucleus, the nucleosome cores are connected by relatively extended DNA linkers forming beads-on-a-string nucleosome arrays. The nucleosome arrays fold into higher-order structures that mediate DNA packing and availability for the DNA recognizing machinery (*7*, *8*). Transcriptionally active chromosomal domains accumulate unconstrained negative supercoiling (*9*, *10*), indicating that active chromatin may have a different linear distribution of torsional stress compared to condensed heterochromatin. These findings necessitate experiments aimed at relating the intrinsic chromatin structural variations predicted in vitro and in silico to DNA topologies and associated functional interactions in vivo.

Monitoring of DNA supercoiling in circular nucleosome arrays (minichromosomes) by topological gel assays has long been used to analyze topological properties of DNA in chromatin. These assays are based on the helical periodicity of DNA making one turn per ~10.5 bp under physiological conditions (*11*, *12*), which corresponds to helical Twist ≈ 34.5°. When the ends of the DNA chains are constrained in covalently closed circular DNA (ccDNA), the changes in the DNA Twist (*Tw*) are compensated by the changes in the Writhe (*Wr*) according to the well-known equation $\Delta Lk = \Delta Tw + Wr$, where the linking number (*Lk*) is defined as the number of times one strand of the duplex turns around the other (*13*–*16*). Note that the three parameters describing the DNA topology (ΔLk, ΔTw, and *Wr*) are measured relative to the relaxed state of DNA. Therefore, $\Delta Wr = Wr$ because the Writhe of unconstrained DNA is zero.

For a chain of nucleosomes, the x-ray crystal structure of the nucleosome core (*1*–*3*) predicts the generation of DNA supercoiling with $Wr = \Delta Lk = -1.7$ per nucleosome if the DNA Twist is not changed ($\Delta Tw = 0$). However, multiple measurements of ΔLk in ccDNA from either native minichromosomes of SV40 virus (*17*, *18*) or nucleosome arrays reconstituted from histones and circular DNA (*19*) persistently resulted in experimental values of $\Delta Lk = -1.0$. This discrepancy is known as the linking number paradox (*16*, *20*–*22*). When acetylated histones were used for reconstitution, the linking number changed to $\Delta Lk = -0.8$ (*23*), which is consistent with contribution of the nucleosome core structure to the associated DNA topology, according to the surface linking theory (*24*).

How could the nucleosome structure and topological properties of the nucleosome chain be reconciled? One explanation is that the DNA Twist in the nucleosome cores could differ from that of naked DNA in solution (*20*–*22*, *24*–*27*). The other possibility is that a special path of linker DNA could alter Writhe (*15*, *28*). Specific linker DNA geometries consistent with the observed DNA topology have been proposed (*28*–*33*). However, the actual linker DNA path within topologically constrained chromatin domains remained obscure because of the absence of adequate circular minichromosome models with precise nucleosome positions.

During the past dozen years, there has been a significant progress in the structural studies of chromatin, largely due to a wide usage of strongly positioned "601" nucleosome sequence (*34*). In particular, the seminal studies of Richmond and colleagues showed the two-start zigzag fibers in solution (*35*) and in crystal form (*36*). Their results, together with the high-resolution cryo-electron microscopy (cryo-EM) data obtained by Song *et al.* (*37*), strongly support the two-start zigzag organization of chromatin fibers for relatively short nucleosome repeat lengths (NRLs) = 167, 177, and 187 bp. In addition, the EM images presented by Rhodes and co-workers (*38*) confirmed zigzag organization for NRL = 167 bp, whereas for NRL = 197 bp and longer, more tightly packed fibers were observed, especially in the presence of linker histones.

[1]Laboratory of Cell Biology, Center for Cancer Research, National Cancer Institute, National Institutes of Health, Bethesda, MD 20892, USA. [2]Department of Biochemistry and Molecular Biology, Pennsylvania State University College of Medicine, Hershey, PA 17033, USA.
*Corresponding author. Email: sag17@psu.edu (S.A.G.); zhurkin@nih.gov (V.B.Z.)

All these structures were obtained for arrays of strongly positioned 601 nucleosomes (*34*), with NRL varying from 167 to 237 bp in increments of 10 bp. Provided that the nucleosome core is 147 bp (*2*), the linker length L varies from 20 to 90 bp, that is, L belongs to the $\{10n\}$ series. On the other hand, it is known that in vivo, the linker sizes are close to $\{10n + 5\}$ values (*39*–*42*). Thus, the structural data mentioned above correspond to linker lengths with occurrences in vivo that are relatively small.

Recently, we have both experimentally and theoretically analyzed positioned nucleosomal arrays (NAs) with linker lengths belonging to the $\{10n\}$ and $\{10n + 5\}$ series. Using analytical ultracentrifugation and EM imaging, we demonstrated that fibers with $L = 25$ bp have less propensity to fold in a compact state than those with $L = 20$ or 30 bp (*43*). Furthermore, using computer modeling, we predicted the two families of energetically stable conformations of the two-start zigzag fibers, one with $L = 10n$ and the other with $L = 10n + 5$ to be topologically different, the former imposing ~50% higher absolute $|\Delta Lk|$ values in the circular DNA (see Fig. 1) (*44*, *45*). Here, we experimentally addressed these predictions for circular nucleosome arrays containing regularly spaced repeats of the 601 nucleosome positioning sequence (*34*).

RESULTS

Plasmid-based DNA circles

We prepared circular DNA templates using two different methods. First, we constructed plasmid-based DNA circles containing 12 repeats, the 601 sequence with NRL = 167 or 172 bp inserted into pUC19 vector (see Materials and Methods). In these 4.7-kb-long circles, about half of DNA belongs to pUC19 vector, which is not a nucleosome positioning sequence. To ensure that the presence of vector DNA does not affect the resulting measurements of ΔLk difference, we also prepared DNA minicircles consisting purely of 601 repeats (see below).

The plasmid-based circular constructs (denoted p-167x12 and p-172x12) were prepared by standard methods of cell transformation, DNA extraction, and purification (see Materials and Methods). Plasmid DNA extracted from cells has a superhelical density $\sigma \approx -0.06$ (*46*), which is expected to facilitate the formation of nucleosomes. Therefore, we used these plasmid-based circles for reconstitution of nucleosomes by a standard salt dialysis method. Examination of the resulting NAs by electrophoretic mobility retardation assay on native agarose gel (fig. S1) shows practically complete incorporation of DNA into the nucleosome bands at the 100% loading of the core histones. We also digested the NAs with restriction enzymes to mononucleosomes and verified the equal core histone loading by the nucleosome band shift assay (fig. S2A).

Next, DNA in the reconstituted NAs was relaxed with topoisomerase I (Topo I), deproteinized, and run on agarose gels containing different concentrations of intercalator chloroquine (CQ). Comparison of the electrophoretic mobility of supercoiled circular DNA (scDNA) obtained with variable histone loading allows monitoring increase in the superhelical density of DNA that accompanies the formation of nucleosomes (Fig. 2). Our approach is illustrated in fig. S3.

As follows from Fig. 2A (lanes 1 and 2), both DNA circles, p-167x12 and p-172x12 (without core histones), are relaxed and run at the top of the gel. A gradual increase in the core histone loading increases the superhelical density and accordingly changes the electrophoretic mobility, entirely consistent with the scheme shown in fig. S3. Specifically, the DNA samples obtained with 25% loading of histones have a "modest" superhelical density (Fig. 2A, lanes 4 and 5), which is increased at 50 to 75% loading, as reflected in a relatively high gel mobility (lanes 6 to 9). Finally, the 100% loading of core histones further increases superhelical density of DNA, so that the tightly coiled DNA migrates to the very bottom of the gel and forms zones of poorly resolved bands (Fig. 2A, lanes 10 and 11).

To resolve individual fast-migrating bands, we repeated the electrophoresis in the presence of various concentrations of CQ, which is known to induce additional positive supercoils in circular DNA (*47*). The DNA circles obtained with a small loading of histones (0 and 25%) become positively supercoiled and run at the bottom of the gel [Fig. 2, B (lanes 1 and 2) and C (lanes 1, 2, 4, and 5)]. The DNA purified from NAs with 50 to 75% loading has intermediate superhelical density; its gel mobility is reversed in the presence of CQ [Fig. 2, B (lanes 6 and 7) and C (lanes 6 to 9)], in agreement with published data (*48*). For DNA with the highest superhelical density (with 100% histone loading) in the presence of CQ (1.5 μg/ml), we observed a strong decrease in mobility so that individual bands can be resolved on the gel (Fig. 2B, lanes 10 and 11).

Now, using gels shown in Fig. 2B (CQ = 1.5 μg/ml), we can accurately determine the change in the DNA linking number induced by the formation of nucleosomes. On the basis of the analysis presented above, we conclude that, for the low histone loading (0 and 25%), the p-167x12 and p-172x12 constructs have similar number of positive superhelical turns. The dominant topoisomers are either located at the same position,

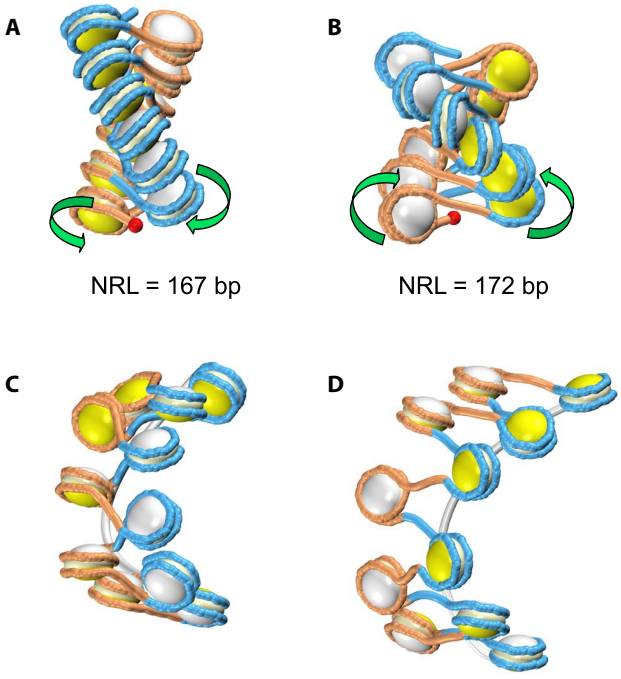

Fig. 1. Models of two-start chromatin fibers with NRLs = 167 and 172 bp. (**A** and **B**) Energy-optimized regular fibers (*43*, *44*) containing 12 nucleosomes, with NRL = 167 bp (A) and NRL = 172 bp (B). The DNA linking number per nucleosome, $\Delta Lk = -1.37$ and -0.93, respectively. The DNA is shown in alternating blue and orange colors to emphasize the two stacks of nucleosomes; the DNA "entry" points are shown as red balls. The histone cores are shown in two colors—The entry sides are in yellow, and the "exit" sides are in white. In this manner, it is easier to distinguish the fiber configurations. In addition, the green arrows indicate different DNA folding pathways in the two topoisomers. (**C** and **D**) Representative configurations of the 167x11 and 172x11 circular NAs obtained during Monte Carlo simulations (see main text and Fig. 3 for details). Note that the circular topoisomers (C and D) are significantly distorted and extended compared to the regular conformers (A and B). The nucleosome-free DNA fragments are shown as white tubes.

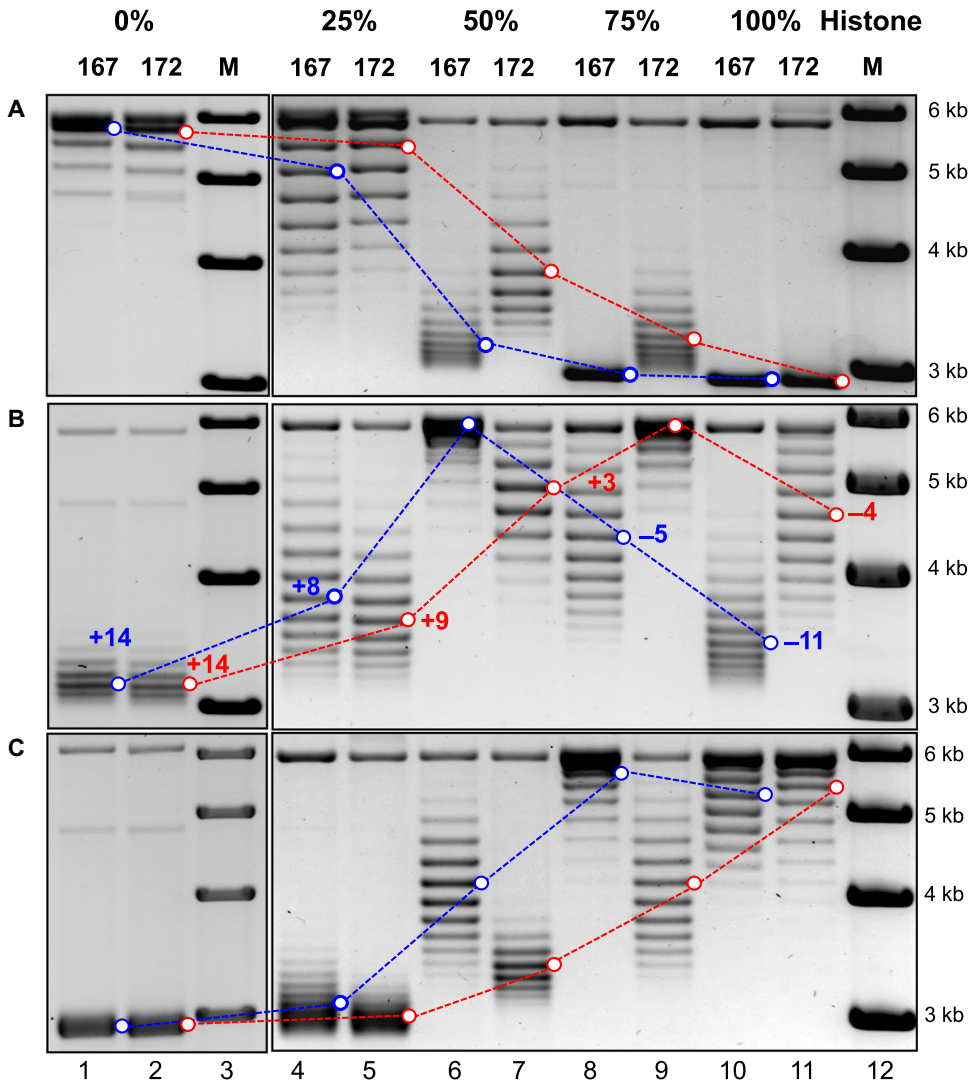

Fig. 2. Topological difference between NAs with 167- and 172-bp NRLs reconstituted on plasmid DNA. Plasmid-based circular DNA templates p-167x12 (lanes 1, 4, 6, 8, and 10) and p-172x12 (lanes 2, 5, 7, 9, and 11) were reconstituted with 0, 25, 50, 75, and 100% core histones (top), treated with Topo I, and the circular DNA was isolated and separated on agarose gels run in the absence (**A**) and presence of CQ (1.5 μg/ml) (**B**) and CQ (4.0 μg/ml) (**C**) in the gel and TAE buffer. Lanes 3 and 12 show molecular weight markers. The strongest bands are indicated by blue circles for the 167-bp NRL and by red circles for the 172-bp NRL. The numbers of superhelical turns in the topoisomers corresponding to these bands are given in the same colors (B). In particular, for the bands denoted +8 and +9 (lanes 4 and 5), the shifts from the top of the gel (nicked circles, form II) are counted directly. For the bands denoted +14 (lanes 1 and 2), the shift from the top is evaluated from the relative shift of six supercoils between these bands and the band +8 (lane 4). Difference in DNA linking number between the 167- and 172-bp NRL constructs, or $\Delta(\Delta Lk)$, equals 1 at 25%, 5 at 50%, 6 at 75%, and 7 at 100% loading of core histones. Note that the presence of intercalator CQ introduces additional positive supercoils in DNA and changes its electrophoretic mobility. For example, the DNA circles relaxed in the absence of histones (lanes 1 and 2) become strongly supercoiled and run at the bottom of the gel. By contrast, the strong negative superhelical density of DNA obtained at 100% loading of histones (lanes 10 and 11) is partially compensated by CQ, and thus, its mobility is decreased (see fig. S3 for details).

band +14 (lanes 1 and 2), or shifted by one band (lanes 4 and 5; bands +8 and +9). For the 100% loading, both DNA circles, p-167x12 and p-172x12, have negative superhelical turns and now show a marked difference between the two samples. Evaluation of the linking number difference between the p-167x12 and p-172x12 nucleosome arrays is straightforward and gives a change of $\Delta\Delta Lk = 7$ negative supercoils in 167-bp versus 172-bp arrays. In the cases of 50 and 75% loadings (lanes 6 and 9), the strongest bands are located too close to the top of the gels, and it is impossible to decide whether they correspond to the negative or positive supercoils from the one-dimensional (1D) gels.

To resolve all topoisomers on a single gel, we run 2D electrophoreses (fig. S4). The CQ concentrations were selected so that the strongest bands for the p-172x12 construct would be located at the top of the gel, and for the p-167x12 construct, they would be on the left side of the gel. As a result, we find that the dominant topoisomers in the two constructs are shifted by 5 to 6 supercoils for 50% histone loading (fig. S4A) and by 6 to 7 supercoils for 75% loading (fig. S4B). Thus, we conclude that the topological difference between the p-167x12 and p-172x12 constructs, $\Delta\Delta Lk$, monotonically increases, reaching about seven supercoils when the loading of core histones increases to 100%.

Provided that the nucleosome arrays have the same number of 601 nucleosomes and the vector-associated nucleosomes are not supposed to change between the two samples, our data are consistent with the model-predicted (Fig. 1) difference in $\Delta\Delta Lk = 0.5$ (per 601 nucleosome) between the p-167x12 and p-172x12 constructs.

DNA minicircles

To ensure that the *Lk* difference between the two types of chromatin fibers observed above is not affected by the presence of vector DNA, we analyzed DNA minicircles containing only the 601 repeats. This approach is similar to that previously used in construction of the minicircles based on sea urchin 5*S* DNA nucleosome positioning sequences by Simpson *et al.* (*19*) and Norton *et al.* (*23*). The 2-kb-long supercoiled DNA circles were prepared by ligation and relaxation by Topo I in the presence of various concentrations of ethidium bromide (EtBr) (see Materials and Methods), which allowed to produce scDNA with defined superhelical density (*49*). By gradually increasing concentration of EtBr up to 2.0 μg/ml and comparing electrophoretic mobility of scDNA in the presence of variable amounts of CQ, we were able to modulate the number of supercoils in each sample (fig. S5). In particular, the scDNA obtained in the presence of EtBr (2.0 μg/ml) has 12 negative supercoils (fig. S5D), which corresponds to a superhelical density $\sigma = -0.06$ in the 2-kb-long minicircle [note that this superhelical density is comparable to that in native *Escherichia coli* plasmids (*46*)]. The 167x12 and 172x12 minicircles produced the same superhelical density (172x12 bands are shown as asterisks in fig. S5). We used 167x12 scDNA as a reference for measuring the number of DNA supercoils in scDNA extracted from the NAs.

Reconstitution of nucleosomes on the scDNA formed in the presence of EtBr (2.0 μg/ml) gave a result very similar to that in the case of the plasmid-based circles, namely DNA in 167x12 NAs is more negatively supercoiled than that in 172x12 NAs (Fig. 3, A and B). However, the topological difference ($\Delta\Delta Lk$) between the two arrays is only three supercoils. In addition, the number of DNA supercoils in these arrays (11 and 8 supercoils, respectively) is less than expected for complete nucleosome saturation (Fig. 3, A and B). This result is consistent with the number of nucleosomes directly counted on the EM micrographs (Fig. 3, C and D, and the supplementary EM data set file (pdf). Instead of 12 nucleosomes expected for the 100% loading of core histones, only about nine nucleosomes, on average, are formed on both constructs, 167x12 and 172x12 (Fig. 3, C and D). Most likely, the limited number of nucleosomes formed on the 2-kb-long circles is due to the decreased conformational flexibility of DNA during nucleosome reconstitution in the minicircles (compared to the 4.7-kb-long plasmid-based circles).

To facilitate the formation of nucleosomes, we increased the number of negative supercoils in minicircular DNA using scDNA prepared in the presence of EtBr (4.0 μg/ml) and maintaining equal distribution of superhelical topoisomers between the two constructs (fig. S6). The efficient saturation of the DNA minicircles by histones was confirmed by Nla III restriction digestion assay excising equal ratios of occupied nucleosomes from the 167 and 172 minicircles at equal histone loading (fig. S2B). As a result, the number of nucleosomes detectable on the EM micrographs increased to ~11, on average, the distribution of the corresponding numbers narrowed, and the minicircles containing the full amount of 12 nucleosomes became rather abundant (Fig. 3, G and H). Accordingly, the number of supercoils increased up to 15 and 10 for NRLs = 167 and 172 bp, respectively (Fig. 3, E and F). For illustration, the representative conformations of 167x11 and 172x11 NAs obtained in the course of energy minimization are shown in Fig. 1 (C and D).

Note that the average numbers of nucleosomes in the 167-bp NRL arrays (10.86) and in the 172-bp NRL arrays (10.94) are virtually equal (Fig. 3G); therefore, we can exclude the possibility that the stronger superhelical density observed for NRL = 167 bp is the result of the higher histone loading in this case. Thus, the topological difference between the uniform {10*n*} and {10*n* + 5} NAs increased to five supercoils, or 45% of the total number of nucleosomes, in excellent agreement with our model (Fig. 1) predicting the dependence of the nucleosome array folding and topology on the linker DNA length.

Previously, in similar experiments with minicircular reconstitutes of 207-bp NRL sea urchin 5*S* DNA nucleosomes, it had been shown that the reconstitution persistently resulted in experimental values of $\Delta Lk = -1.01$ (±0.08) (*19*). Consistent with this result, we found here that, in minicircular DNA containing 12 repeats of 601 nucleosome positioning sequence with NRL = 207 bp, the ΔLk change was about −1.1 (figs. S7 and S8). We also observed that reconstitution of nucleosomes on another minicircular DNA construct with NRL = 188 bp brought changes of $\Delta Lk \approx -1.3$. Thus, we see that, in the three NAs belonging to the {10*n*} series, 12x167, 12x188, and 12x207, the absolute value of DNA linking number, $|\Delta Lk|$, gradually decreases from 1.4 to 1.1 with increase in the linker length, in a good agreement with our predictions based on energy minimization of the fiber topoisomers (fig. S9) (*45*).

DISCUSSION

Our results reconcile the nucleosome core crystal structure with topology of the nucleosome array. For the first time, we show that the level of DNA supercoiling in the NAs varies by as much as ~50% depending on the DNA linker length. The DNA linking number per nucleosome, ΔLk, changes from −1.4 for L = 20 bp to −0.9 for L = 25 bp (in DNA minicircles consisting purely of 601 repeats). Here, like in the previous nucleosome minicircle reconstitution experiments (*19*, *23*), the negative supercoiling of template DNA was used to promote histone octamer assembly efficiency. Our results show that the number of assembled nucleosomes is equal for minicircles with equal number of nucleosome templates and initial supercoiling, although the resulting numbers of unconstrained supercoils are different. Thus, the observed ΔLk changes are due to the changes in the nucleosome linker length rather than initial supercoiling density or the number of nucleosomes. Because the same sequence 601 was used in both cases, one can be certain that the observed change in DNA supercoiling is due to the changes in the global DNA pathway (Writhe) rather than to the alteration of DNA twisting in nucleosomes. Note that the nucleosome positioning signals embedded in this sequence are so strong that they secure the same positioning of the 601 nucleosomes both in array and in a single nucleosome with a single-nucleotide precision (*50*, *51*). Furthermore, changing the DNA linker length in the 601 repeats is sufficient to significantly alter the overall DNA topology in hybrid plasmids containing a mixture of positioned and nonpositioned nucleosomes and thus mimicking native NAs.

By showing that altered linker spacing is sufficient to change the DNA topology in circular minichromosomes, our results provide a decisive proof to the notion that the chromatin higher-order structure is defined by nucleosome rotational settings (*43*, *44*). Previous crystallographic and EM studies of Richmond and colleagues (*35*, *36*), together with the high-resolution cryo-EM data (*35*), revealed the two-start zigzag organization of chromatin fibers for the linkers belonging to the {10*n*} series (L = 20, 30, and 40 bp). Overall, the DNA folding in these fibers remains the same, the main difference being gradual monotonic changes in dimensions of fibers due to increase in linker length. By

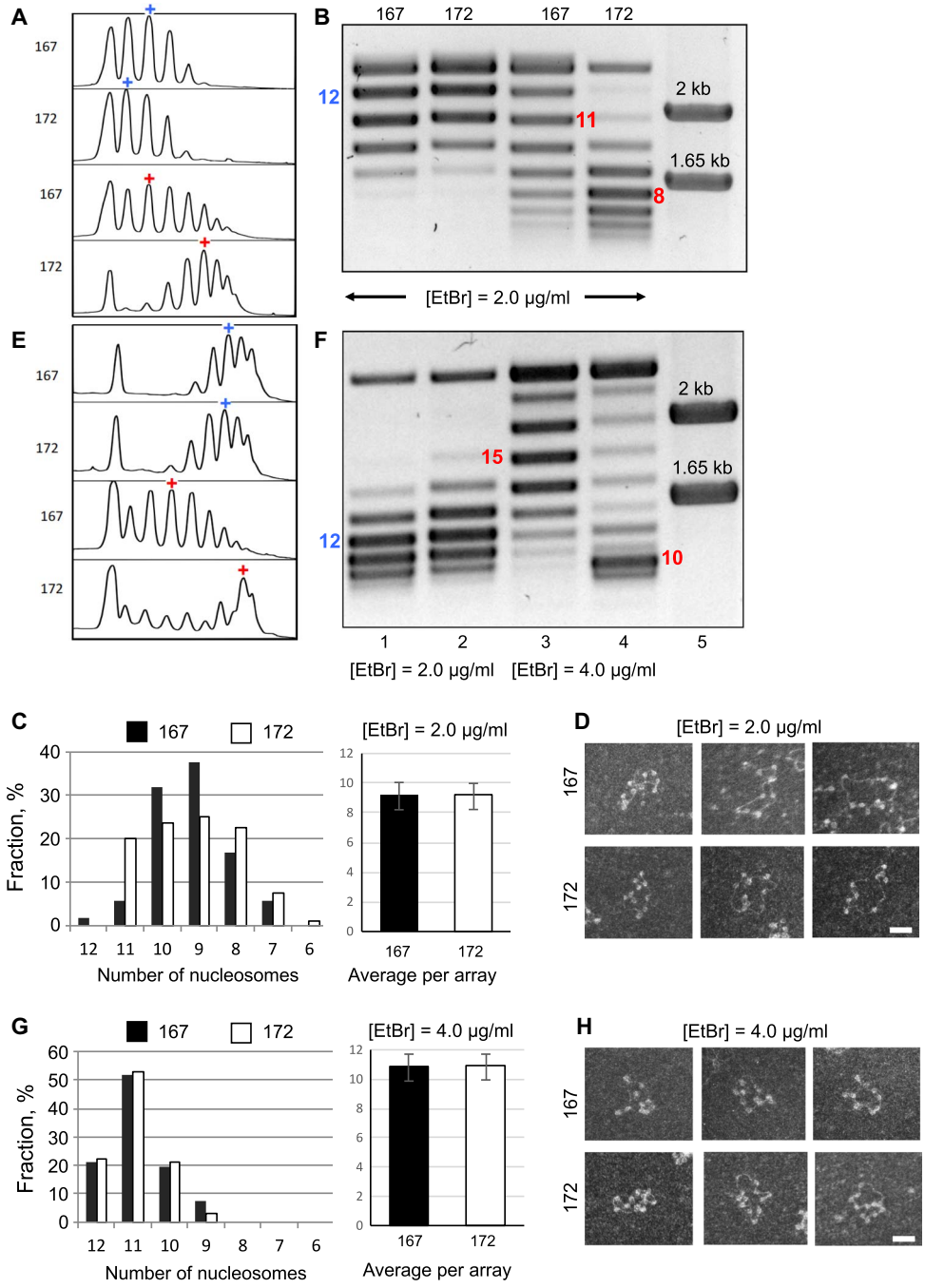

Fig. 3. Topological difference between 167x12 and 172x12 NAs reconstituted on minicircular DNA. Nucleosomes were reconstituted on the scDNA templates prepared in the presence of EtBr (2 μg/ml) (**A** to **D**) and EtBr (4 μg/ml) (**E** to **H**). (A and E) Scans of gels in (B) and (F). The strongest bands are marked with "+". (B and F) Electrophoretic mobility of the DNA topoisomers extracted from NAs was compared with the mobility of scDNA templates obtained at [EtBr] = 2 μg/ml (lanes 1 and 2). Gels were run in the presence of CQ (8 μg/ml) (B) and CQ (32 μg/ml) (F). Lane 5 shows molecular weight markers. Note that the scDNAs with 167-bp (lane 1) and 172-bp (lane 2) NRLs have similar distributions of topoisomers, with the strongest bands corresponding to $\Delta Lk = -12$ (fig. S5D). NAs reconstituted on these scDNAs (obtained at [EtBr] = 2 μg/ml) have $\Delta Lk = -11$ and -8 (lanes 3 and 4) (B). Arrays reconstituted on scDNA obtained at [EtBr] = 4 μg/ml have $\Delta Lk = -15$ and -10 (lanes 3 and 4) (F). (C and G) Graphs showing the average number of nucleosomes (10.9) on 167x12 and 172x12 arrays and distributions of the number of nucleosomes per one minicircle (calculated from EM_images_interactive PDF file). Normalization of the values $\Delta Lk = -15$ and -10 [shown in (F)] gives the DNA linking number per nucleosome, $\Delta Lk = -1.38$ and -0.92 for the 167x12 and 172x12 arrays, respectively. (D and H) Representative transmission EM images of relaxed minicircular 167x12 and 172x12 arrays reconstituted on scDNA obtained at [EtBr] = 2 μg/ml (D) and [EtBr] = 4 μg/ml (H). Scale bars, 50 nm.

contrast, we observe here an abrupt change in DNA topology when comparing the fibers with L = 20 and 25 bp, consistent with the folding trajectories of DNA linkers being markedly different in the two cases (Fig. 1). The topological polymorphism of a chromatin fiber depending on linker DNA trajectory, first noted by Crick (*15*), is reflected in the early studies by Worcel *et al.* (*30*), Woodcock *et al.* (*31*), and Williams *et al.* (*32*) who presented space-filling models of the chromatin fiber with the DNA linking number ΔLk varying from −1 to −2 per nucleosome, depending on the DNA trajectory.

The increased fiber "plasticity" observed for the {10n + 5} linkers (*43*–*45*) is biologically relevant because the {10n + 5} values are frequently found in vivo (*39*–*43*). On the other hand, the more tightly folded {10n} structures appear to facilitate nucleosome disk stacking by interactions between histone H4 N-terminal domain and histone H2A/H2B acidic patch at the nucleosomal interface (*35*) and make the structure to be especially sensitive to the effects of histone H4 acetylation (*52*).

The experimentally observed topological polymorphism and an extrapolation of our model to include a wide range of variations of linker lengths provide a simple explanation for the observed DNA linking number $\Delta Lk \approx -1.0$ in native SV40 minichromosomes (*17*, *18*). These minichromosomes do not have a strong nucleosome positioning and thus may give rise to ΔLk values widely distributed between −0.8 and −1.5 per nucleosome (fig. S9). For nucleosome linker lengths close to 60 bp (NRL = 207 bp), which is the most common value for eukaryotic chromatin, the mean value of the ΔLk is about −1.05 per nucleosome (fig. S9). Earlier analysis of the distribution of ΔLk for a nucleosome array with randomized nucleosome orientation (*29*) also showed the ΔLk values close to −1 per nucleosome.

In living cells, the DNA-dependent processes, such as transcription, constantly generate positive and negative local DNA supercoiling in accord with the twin-domain model of transcription (*53*). Because Topo I and Topo II do not completely remove this dynamically induced supercoiling, transcriptionally active chromosomal domains accumulate regions with the higher and lower superhelical densities, which can be detected by a combination of psoralen cross-linking with genome-wide sequencing (*9*, *54*, *55*). Recent genome-wide mapping with psoralen revealed extended (on average, 100 kb) overtwisted domains correlated with transcriptional activity and chromatin decondensation (*10*).

In contrast to the transcriptionally active chromatin, transcriptionally silent domains in yeast acquire negative supercoiling (*56*). Our data suggest that the level of DNA supercoiling is closely tied with the nucleosome spacing, so that in the repressed state, the supercoiling could become more negative ($\Delta Lk \approx -1.5$), and the overall chromatin structure could become more compact (Fig. 1A) because of a larger fraction of nucleosomes acquiring the {10n} class of repeats (for example, NRL = 167 bp). This is because, in the nucleosome arrays belonging to the {10n} series, the nucleosome stacking is enhanced by histone H4 N-tail/histone H2A/H2B acidic patch interactions (*1*, *44*).

We believe that our in vitro findings reflect important aspects of chromatin structure adapted to rendering the repressed chromatin more compact by acquiring special nucleosome spacing. More specifically, we propose that, by altering nucleosome spacing, transcription may impose long-lasting topological changes in the nucleosome arrays and thus generate topologically and structurally distinct chromosomal domains of {10n} class of nucleosome repeats that will maintain their more compact and repressed states. Future studies, especially detailed 3D analysis by advanced imaging techniques such as high-resolution cryo-EM tomography, should reveal the actual DNA configurations in active and repressed chromatin.

MATERIALS AND METHODS

Preparation of circular DNA constructs

The plasmid-based DNA circles have 12 repeats of 601 nucleosome positioning sequence with repeat length of either 167 or 172 bp inserted into pUC19 vector (*43*). For the pUC19-167x12 plasmid, additional 60 bp were added to make it the same DNA length as the pUC19-172x12 plasmid. Two self-complementary single-stranded DNA fragments, purchased from Integrated DNA Technologies, were annealed so that the resulting double-stranded DNA (dsDNA) had single-stranded overhangs with Xba I site on one end and Eco RI site on the other. The pUC19-167x12 construct was digested with Eco RI and Xba I restriction enzymes and ligated with dsDNA with overhangs using standard procedures. Ligation products were used to transform Stbl2 competent cells; the transformants were grown, and plasmid DNA was prepared using a plasmid purification kit (Qiagen) according to the manufacturer's instructions.

DNA minicircles containing only 12-mer 601 nucleosomes with repeat lengths of 167, 172, and 207 bp were prepared by ligations of linear DNA fragments at low concentration to ensure circle formation rather than ligation of multiple linear fragments. The (167x12)+60-, 172x12-, and 207x12-bp linear DNA fragments were prepared by cutting off DNA fragments between Xba I and Spe I restriction sites from pUC19 plasmids with corresponding inserts. The DNA fragments were run on 1% agarose gel, bands with inserts were isolated, and DNA was extracted with Promega Wizard SV Gel and PCR Clean-Up System, cleaned with phenol/chloroform, and precipitated. Linear DNA fragments were suspended in 10 mM tris-HCl (pH 7.5). For ligation reaction, DNA was diluted to 1 ng/μl in a total volume of 800 μl in multiple tubes. A total of 3200 units of T4 ligase (New England Biolabs) were added to each tube. Reaction was kept at 16°C for about 48 hours. Every 2 to 3 hours, additional 800 ng of DNA was added to each reaction mixture. Ligation mixtures were concentrated and washed in 10 mM tris-HCl (pH 7.5) using Amicon Ultra-4 centrifugal filters units with a molecular mass cutoff of 100 K.

To prepare scDNA with defined superhelical densities (*49*), 3 μg of DNA samples were treated with various concentrations of EtBr in the presence of 10 units of human Topo I (cat. no. TG2005H, TopoGEN) in Topo I buffer [10 mM tris-HCl (pH 7.9), 1 mM EDTA, 150 mM NaCl, 0.1% bovine serum albumin (BSA), 0.1 mM spermidine, and 5% glycerol]. Mixtures were kept at 37°C for 2 hours. The reaction was stopped by the addition of Na acetate to 0.33 M, and samples were cleaned with phenol/chloroform. After precipitation, scDNA was suspended in 10 mM tris-HCl (pH 7.5).

Preparation of circular NAs

NAs were reconstituted by mixing purified chicken erythrocyte core histones (*57*, *58*) with circular DNA. The reconstitution was performed as described (*43*) by a salt dialysis from 2.0 to 0.5 M NaCl, followed by dialysis to 10 mM NaCl, 10 mM tris-HCl (pH 8.0), and 0.25 mM EDTA.

For Topo I treatment, 1 μg of NAs was mixed with 10 units of Topo I in Topo I buffer in 50-μl reaction volume for 30 min at 37°C. The core histones were then removed by SDS/proteinase K treatment, and DNA was cleaned with Promega Wizard SV Gel and PCR Clean-Up System. DNA samples were run on 1% agarose gels containing different concentrations of CQ in tris-acetate-EDTA (TAE) buffer.

Restriction enzyme digestion assay

The plasmid-based circular NAs were diluted to 40 μg/ml in a 40-μl reaction buffer [50 K acetate, 20 mM tris-acetate (pH 7.9), 1 mM Mg

acetate, and BSA (100 μg/ml)] and digested with the mixture of restriction enzymes (Xba I, Spe I, and Nla III), 20 units each, overnight at 37°C. Reaction was stopped by the addition of 10 mM EDTA. The minicircular arrays were digested in the same buffer with restriction enzyme Nla III only. Samples were run on a type IV agarose gel for 2 hours 20 min at 80 V/cm in a horizontal gel electrophoresis apparatus with constant buffer recirculation.

2D electrophoresis

Gels were run in 1% agarose at 3 V/cm for 18 hours in TAE buffer with CQ concentration as indicated. The gels were removed, soaked for 3 hours in TAE buffer with appropriate CQ concentration, placed into e/f apparatus perpendicular to the first direction, and run again for 18 hours at 3 V/cm. Gels were stained in GelRed stain (cat. no. 41002, Biotium) and visualized using Bio-Rad Image Lab imager.

Transmission EM of NAs

For EM, the reconstituted and Topo I–treated nucleosome arrays were dialyzed in 10 mM Hepes, 10 mM NaCl, and 0.1 mM EDTA buffer for 4 hours and then fixed with 0.1% glutaraldehyde overnight at +4°C. Glutaraldehyde was then removed by dialysis in the same buffer (without glutaraldehyde). Samples were diluted with 50 mM NaCl to ~1 μg/ml, applied to carbon-coated and glow-discharged EM grids (T1000-Cu, Electron Microscopy Science), and stained with 0.04% aqueous uranyl acetate, as previously described (*43*). Dark-field images were obtained and digitally recorded as described using JEM-1400 electron microscope (JEOL USA) at 120 kV with SC1000 Orius 11-megapixel charge-coupled device camera (Gatan Inc.). The number of nucleosomes formed in each array was counted as described (*50*). Electron micrographs of individual particles and the overlaying counting masks are included in the layered EM data set file (pdf). The counting masks can be easily removed from the view using free Adobe Acrobat Reader DC software (https://acrobat.adobe.com/us/en/products/pdf-reader.html) or any other Adobe Acrobat version that supports layered PDF documents.

SUPPLEMENTARY MATERIALS

Supplementary material for this article is available at http://advances.sciencemag.org/cgi/content/full/3/10/e1700957/DC1

fig. S1. Analysis of circular nucleosome array reconstitution by electrophoretic mobility shift assay.

fig. S2. Analysis of circular nucleosome array reconstitution by restriction enzyme digestion and electrophoretic DNA band-shift assay.

fig. S3. Binding of intercalator CQ to supercoiled DNA changes its electrophoretic mobility.

fig. S4. 2D gel electrophoresis of DNA extracted from NAs with 167- and 172-bp NRLs.

fig. S5. Modulating negative supercoiling in DNA minicircles in the presence of various concentrations of EtBr.

fig. S6. Preparation of supercoiled DNA constructs 167x12 and 172x12 relaxed by Topo I in the presence of EtBr (4.0 μg/ml).

fig. S7. Negative supercoiling of DNA minicircles with 207-bp NRL in the presence of EtBr.

fig. S8. Negative supercoiling of circular NAs with 207-bp NRL.

fig. S9. Linking number per nucleosome, ΔLk, in regular fibers with various linker lengths.

EM data set file (pdf)

REFERENCES AND NOTES

1. K. Luger, A. W. Mäder, R. K. Richmond, D. F. Sargent, T. J. Richmond, Crystal structure of the nucleosome core particle at 2.8 Å resolution. *Nature* **389**, 251–260 (1997).
2. C. A. Davey, D. F. Sargent, K. Luger, A. W. Mäder, T. J. Richmond, Solvent mediated interactions in the structure of the nucleosome core particle at 1.9 Å resolution. *J. Mol. Biol.* **319**, 1097–1113 (2002).
3. M. S. Ong, T. J. Richmond, C. A. Davey, DNA stretching and extreme kinking in the nucleosome core. *J. Mol. Biol.* **368**, 1067–1074 (2007).
4. G. Felsenfeld, M. Groudine, Controlling the double helix. *Nature* **421**, 448–453 (2003).
5. R. D. Kornberg, Y. Lorch, Chromatin rules. *Nat. Struct. Mol. Biol.* **14**, 986–988 (2007).
6. C. Jiang, B. F. Pugh, Nucleosome positioning and gene regulation: Advances through genomics. *Nat. Rev. Genet.* **10**, 161–172 (2009).
7. K. Luger, M. L. Dechassa, D. J. Tremethick, New insights into nucleosome and chromatin structure: An ordered state or a disordered affair? *Nat. Rev. Mol. Cell Biol.* **13**, 436–447 (2012).
8. S. A. Grigoryev, C. L. Woodcock, Chromatin organization—The 30 nm fiber. *Exp. Cell Res.* **318**, 1448–1455 (2012).
9. F. Kouzine, A. Gupta, L. Baranello, D. Wojtowicz, K. Ben-Aissa, J. Liu, T. M. Przytycka, D. Levens, Transcription-dependent dynamic supercoiling is a short-range genomic force. *Nat. Struct. Mol. Biol.* **20**, 396–403 (2013).
10. C. Naughton, N. Avlonitis, S. Corless, J. G. Prendergast, I. K. Mati, P. P. Eijk, S. L. Cockroft, M. Bradley, B. Ylstra, N. Gilbert, Transcription forms and remodels supercoiling domains unfolding large-scale chromatin structures. *Nat. Struct. Mol. Biol.* **20**, 387–395 (2013).
11. D. E. Depew, J. C. Wang, Conformational fluctuations of DNA helix. *Proc. Natl. Acad. Sci. U.S.A.* **72**, 4275–4279 (1975).
12. D. Rhodes, A. Klug, Helical periodicity of DNA determined by enzyme digestion. *Nature* **286**, 573–578 (1980).
13. J. H. White, Self-linking and the Gauss integral in higher dimensions. *Am. J. Math.* **91**, 693–728 (1969).
14. F. B. Fuller, Decomposition of the linking number of a closed ribbon: A problem from molecular biology. *Proc. Natl. Acad. Sci. U.S.A.* **75**, 3557–3561 (1978).
15. F. H. Crick, Linking numbers and nucleosomes. *Proc. Natl. Acad. Sci. U.S.A.* **73**, 2639–2643 (1976).
16. A. Prunell, A topological approach to nucleosome structure and dynamics: The linking number paradox and other issues. *Biophys. J.* **74**, 2531–2544 (1998).
17. W. Keller, Determination of the number of superhelical turns in simian virus 40 DNA by gel electrophoresis. *Proc. Natl. Acad. Sci. U.S.A.* **72**, 4876–4880 (1975).
18. J. E. Germond, B. Hirt, P. Oudet, M. Gross-Bellark, P. Chambon, Folding of the DNA double helix in chromatin-like structures from simian virus 40. *Proc. Natl. Acad. Sci. U.S.A.* **72**, 1843–1847 (1975).
19. R. T. Simpson, F. Thoma, J. M. Brubaker, Chromatin reconstituted from tandemly repeated cloned DNA fragments and core histones: A model system for study of higher order structure. *Cell* **42**, 799–808 (1985).
20. J. T. Finch, L. C. Lutter, D. Rhodes, R. S. Brown, B. Rushton, M. Levitt, A. Klug, Structure of nucleosome core particles of chromatin. *Nature* **269**, 29–36 (1977).
21. J. H. White, W. R. Bauer, The helical repeat of nucleosome-wrapped DNA. *Cell* **56**, 9–10 (1989).
22. A. Klug, A. A. Travers, The helical repeat of nucleosome-wrapped DNA. *Cell* **56**, 10–11 (1989).
23. V. G. Norton, B. S. Imai, P. Yau, E. M. Bradbury, Histone acetylation reduces nucleosome core particle linking number change. *Cell* **57**, 449–457 (1989).
24. W. R. Bauer, J. J. Hayes, J. H. White, A. P. Wolffe, Nucleosome structural changes due to acetylation. *J. Mol. Biol.* **236**, 685–690 (1994).
25. A. Prunell, R. D. Kornberg, L. C. Lutter, A. Klug, M. Levitt, F. H. C. Crick, Periodicity of deoxyribonuclease I digestion of chromatin. *Science* **204**, 855–858 (1979).
26. J. J. Hayes, D. J. Clark, A. P. Wolffe, Histone contributions to the structure of DNA in the nucleosome. *Proc. Natl. Acad. Sci. U.S.A.* **88**, 6829–6833 (1991).
27. A. Klug, L. C. Lutter, The helical periodicity of DNA on the nucleosome. *Nucleic Acids Res.* **9**, 4267–4283 (1981).
28. R. H. Morse, R. T. Simpson, DNA in the nucleosome. *Cell* **54**, 285–287 (1988).
29. S. A. Grigoryev, L. B. Ioffe, The dependence of the linking number of a circular minichromosome upon the shape and the orientation of its nucleosomes. *FEBS Lett.* **130**, 43–46 (1981).
30. A. Worcel, S. Strogatz, D. Riley, Structure of chromatin and the linking number of DNA. *Proc. Natl. Acad. Sci. U.S.A.* **78**, 1461–1465 (1981).
31. C. L. Woodcock, L. L. Frado, J. B. Rattner, The higher-order structure of chromatin: Evidence for a helical ribbon arrangement. *J. Cell Biol.* **99**, 42–52 (1984).
32. S. P. Williams, B. D. Athey, L. J. Muglia, R. S. Schappe, A. H. Gough, J. P. Langmore, Chromatin fibers are left-handed double helices with diameter and mass per unit length that depend on linker length. *Biophys. J.* **49**, 233–248 (1986).
33. A. Stein, DNA wrapping in nucleosomes: The linking number problem re-examined. *Nucleic Acids Res.* **8**, 4803–4820 (1980).
34. P. T. Lowary, J. Widom, New DNA sequence rules for high affinity binding to histone octamer and sequence-directed nucleosome positioning. *J. Mol. Biol.* **276**, 19–42 (1998).
35. B. Dorigo, T. Schalch, A. Kulangara, S. Duda, R. R. Schroeder, T. J. Richmond, Nucleosome arrays reveal the two-start organization of the chromatin fiber. *Science* **306**, 1571–1573 (2004).
36. T. Schalch, S. Duda, D. F. Sargent, T. J. Richmond, X-ray structure of a tetranucleosome and its implications for the chromatin fibre. *Nature* **436**, 138–141 (2005).
37. F. Song, P. Chen, D. Sun, M. Wang, L. Dong, D. Liang, R.-M. Xu, P. Zhu, G. Li, Cryo-EM study of the chromatin fiber reveals a double helix twisted by tetranucleosomal units. *Science* **344**, 376–380 (2014).

38. A. Routh, S. Sandin, D. Rhodes, Nucleosome repeat length and linker histone stoichiometry determine chromatin fiber structure. *Proc. Natl. Acad. Sci. U.S.A.* **105**, 8872–8877 (2008).
39. D. Lohr, K. E. Van Holde, Organization of spacer DNA in chromatin. *Proc. Natl. Acad. Sci. U.S.A.* **76**, 6326–6330 (1979).
40. F. Strauss, A. Prunell, Organization of internucleosomal DNA in rat liver chromatin. *EMBO J.* **2**, 51–56 (1983).
41. K. Brogaard, L. Xi, J.-P. Wang, J. Widom, A map of nucleosome positions in yeast at base-pair resolution. *Nature* **486**, 496–501 (2012).
42. L. N. Voong, L. Xi, A. C. Sebeson, B. Xiong, J.-P. Wang, X. Wang, Insights into nucleosome organization in mouse embryonic stem cells through chemical mapping. *Cell* **167**, 1555–1570.e15 (2016).
43. S. J. Correll, M. H. Schubert, S. A. Grigoryev, Short nucleosome repeats impose rotational modulations on chromatin fibre folding. *EMBO J.* **31**, 2416–2426 (2012).
44. D. Norouzi, V. B. Zhurkin, Topological polymorphism of the two-start chromatin fiber. *Biophys. J.* **108**, 2591–2600 (2015).
45. D. Norouzi, A. Katebi, F. Cui, V. B. Zhurkin, Topological diversity of chromatin fibers: Interplay between nucleosome repeat length, DNA linking number and the level of transcription. *AIMS Biophys.* **2**, 613–629 (2015).
46. F. H. C. Crick, J. H. White, W. R. Bauer, Supercoiled DNA. *Sci. Am.* **243**, 118–133 (1980).
47. M. Shure, D. E. Pulleyblank, J. Vinograd, The problems of eukaryotic and prokaryotic DNA packaging and in vivo conformation posed by superhelix density heterogeneity. *Nucleic Acids Res.* **4**, 1183–1205 (1977).
48. R. R. Sinden, *DNA Structure and Function* (Academic Press, 1984), pp. 129–132.
49. C. K. Singleton, R. D. Wells, The facile generation of covalently closed, circular DNAs with defined negative superhelical densities. *Anal. Biochem.* **122**, 253–257 (1982).
50. S. A. Grigoryev, G. Arya, S. Correll, C. L. Woodcock, T. Schlick, Evidence for heteromorphic chromatin fibers from analysis of nucleosome interactions. *Proc. Natl. Acad. Sci. U.S.A.* **106**, 13317–13322 (2009).
51. T. Nikitina, D. Wang, M. Gomberg, S. A. Grigoryev, V. B. Zhurkin, Combined micrococcal nuclease and exonuclease III digestion reveals precise positions of the nucleosome core/linker junctions: Implications for high-resolution nucleosome mapping. *J. Mol. Biol.* **425**, 1946–1960 (2013).
52. M. Shogren-Knaak, H. Ishii, J.-M. Sun, M. J. Pazin, J. R. Davie, C. L. Peterson, Histone H4-K16 acetylation controls chromatin structure and protein interactions. *Science* **311**, 844–847 (2006).
53. L. F. Liu, J. C. Wang, Supercoiling of the DNA template during transcription. *Proc. Natl. Acad. Sci. U.S.A.* **84**, 7024–7027 (1987).
54. I. Bermúdez, J. García-Martínez, J. E. Pérez-Ortín, J. Roca, A method for genome-wide analysis of DNA helical tension by means of psoralen–DNA photobinding. *Nucleic Acids Res.* **38**, e182 (2010).
55. R. S. Joshi, B. Piña, J. Roca, Positional dependence of transcriptional inhibition by DNA torsional stress in yeast chromosomes. *EMBO J.* **29**, 740–748 (2010).
56. X. Bi, J. R. Broach, DNA in transcriptionally silent chromatin assumes a distinct topology that is sensitive to cell cycle progression. *Mol. Cell Biol.* **17**, 7077–7087 (1997).
57. G. Meersseman, S. Penning, E. M. Bradbury, Chromatosome positioning on assembled long chromatin. Linker histones affect nucleosome placement on 5 S rDNA. *J. Mol. Biol.* **220**, 89–100 (1991).
58. E. M. Springhetti, N. E. Istomina, J. C. Whisstock, T. Nikitina, C. L. Woodcock, S. A. Grigoryev, Role of the M-loop and reactive center loop domains in the folding and bridging of nucleosome arrays by MENT. *J. Biol. Chem.* **278**, 43384–43393 (2003).

Acknowledgments: We are grateful to D. Clark and F. Kouzine for valuable discussions and to H. Chen for technical assistance with EM conducted at the Penn State Hershey Imaging Facility. **Funding:** This work was supported by Intramural Research Program of the NIH, National Cancer Institute (to V.B.Z.), and NSF grant 1516999 (to S.A.G.). **Author contributions:** S.A.G. and V.B.Z. designed the experiments. T.N. and S.A.G. performed the experiments. D.N. performed the structural computations. T.N., S.A.G., and V.B.Z. wrote the manuscript. All authors discussed the results and commented on the manuscript. **Competing interests:** The authors declare that they have no competing interests. **Data and materials availability:** All data needed to evaluate the conclusions in the paper are present in the paper and/or the Supplementary Materials. Additional data related to this paper may be requested from the authors.

Submitted 27 March 2017
Accepted 27 September 2017
Published 27 October 2017
10.1126/sciadv.1700957

Citation: T. Nikitina, D. Norouzi, S. A. Grigoryev, V. B. Zhurkin, DNA topology in chromatin is defined by nucleosome spacing. *Sci. Adv.* **3**, e1700957 (2017).